Structural Engineering and Mechanics, *Vol. 68, No. 5 (2018) 527-536*
DOI: https://doi.org/10.12989/sem.2018.68.5.527

Numerical study of temperature dependent eigenfrequency responses of tilted functionally graded shallow shell structures

Chandra Mouli B[1a], Ramji K[2b], Vishesh R Kar[3c], Subrata K Panda*[4], Lalepalli Anil K[4d] and Harsh K Pandey[5e]

[1]Department of Mechanical Engineering, RISE Krishna Sai Prakasam Group of Institutions, Ongole, India
[2]Dr. B. R. Ambedkar University, Srikakulam, India
[3]Department of Mechanical Engineering, National Institute of Technology, Jamshedpur, India
[4]Department of Mechanical Engineering, National Institute of Technology, Rourkela, India
[5]Dr. C. V. Raman Institute of Science & Technology, Kargi Road Kota, Bilaspur (CG), India

(Received July 14, 2018, Revised August 4, 2018, Accepted August 9, 2018)

Abstract. The free vibration frequency responses of the graded flat and curved (cylindrical, spherical, hyperbolic and elliptical) panel structures investigated in this research considering the rectangular and tilted planforms under unlike temperature loading. For the numerical implementation purpose, a micromechanical model is prepared with the help of Voigt's methodology via the power-law type of material model. Additionally, to incur the exact material strength, the temperature-dependent properties of each constituent of the graded structure included due to unlike thermal environment. The deformation kinematics of the rectangular/tilted graded shallow curved panel structural is modeled via higher-order type of polynomial functions. The final form of the eigenvalue equation of the heated structure obtained via Hamilton's principle and simultaneously solved numerically using finite element steps. To show the solution accuracy, a series of comparison the results are compared with the published data. Some new results are exemplified to exhibit the significance of power-law index, shallowness ratio, aspect ratio and thickness ratio on the combined thermal eigen characteristics of the regular and tilted graded panel structure.

Keywords: FGM; free vibration; tilted panels; TSDT; thermal field

1. Introduction

The consistent demand for advanced materials in the various engineering field is being witnessed to have better durability and performance of the structure under severe conditions. From last few decades, layered composites are being utilised in many weight-sensitivity industries. But, under critical thermal environment, layered structures demonstrate their incapability of enduring the structural integrity due to the delamination type of failure. Therefore, Japanese space scientists conceptualised an advanced form of the composite, called functionally graded material (FGM), by amalgamating two unlike materials with smooth gradation (Koizumi 1993). Several research articles have already been published in the past to investigate the mechanical structural responses of FGM structures subjected to either individual or the combined loading conditions. In this regard, the nonlinear frequency and dynamic bending responses of FG plate structure under the influence of the unlike temperature loading evaluated by Huang and Shen (2004) using the higher-order shear deformation mid-plane theory (HSDT) including von-Karman strain. Also, the lower-order displacement kinematics say, first-order shear deformation theory (FSDT) implemented by Sundararajan *et al.* (2005) to compute the responses of heated FG plate including the large deformation behaviour. In addition, a series of analysis related to the eigenfrequency responses are reported (Patel *et al.* 2005, Uymaz and Aydogdu 2007, Haddadpour *et al.* 2007 and Pradyumna and Bandyopadhyay 2008) for the variable geometrical configurations (flat and curved panel) using different polynomial based kinematic theories and numerical techniques. Similarly, few models are derived for the frequency analysis extended further to explore the stability behaviour of FG curved panels (Pradyumna and Bandyopadhyay 2008) under the elevated thermal field. Additionally, the linear and the nonlinear eigenfrequency responses of the graded structure for the different geometrical configurations are reported using 3D elastic theory (Santos *et al.* 2009) finite element (FE) method (Talha and Singh 2011) including the analytical technique (Baferani *et al.* 2012) in the framework of variable displacement kinematics (HSDT and Kirchhoff's model).

∗Corresponding author, Associate Professor
E-mail: call2subrat@gmail.com
[a]Assistant Professor
E-mail: badiganti1@gmail.com
[b]Professor
E-mail: ramjidme@gmail.com
[c]Assistant Professor
[d]M. Tech
E-mail: anil7567@gmail.com
[e]Associate Professor
E-mail: harsh25pandey@gmail.com

http://www.techno-press.com/journals/sem&subpage=7
ISSN: 1225-4568 (Print), 1598-6217 (Online)

Likewise, the static and time-dependent deflection values of the FG skew structures are reported using the HSDT kinematics (Taj and Chakraborty 2013) and 3D-elasticity theory (Asemi *et al.* 2014). In addition, the nonlinear frequency responses of the heated FG cylindrical panel structure is examined by Shen and Wang (2014) using the HSDT and von Karman type of large deformation relations. The FSDT type of mid-plane displacement including von Karman nonlinear strain and the local meshless techniques employed by Zhu *et al*. (2014) in combination to investigate the nonlinear thermoelastic responses of the FG plate structure. The differential quadrature method is adopted to investígate various structural responses for different material constituents (FGM, carbón nano tube and concrete) and geometrical configurations including the midplane kinematics (Hajmohammad *et al.* 2018, Hajmohammad *et al.* 2018, Hajmohammad *et al.* 2018, Hajmohammad *et al.* 2018, Amnieh *et al.* 2018, Kolahchi and Cheraghbak 2017, Kolahchi *et al.* 2017, Kolahchi *et al.* 2017, Kolahchi 2017, Zarei *et al.* 2017, Kolahchi *et al.* 2016, Arania and Kolahchi 2016, Kolahchi and Bidgoli 2016, Kolahchi *et al*. 2016). Yousfi *et al.* (2018) examined the free vibration responses of FGM plate analytically using Navier solution and high-order hyperbolic shear deformation theory. Bouiadjra *et al.* (2018) employed a new 3D shear deformation theory to examine the bending behaviour of simply supported FGM plate using Navier solution, analytically. Ghannadpour and Kiani (2018) proposed a spectral collocation approach using Legendre basis function to investigate the nonlinear behaviour of FG plates. Pathak *et al.* (2018) developed a novel and simple finite element approach to examine the concrete beam strength by introducing the fiber-reinforced polymer reinforcement. Kiani *et al.* (2016) used Ritz method to investigate the free vibration of a skew FG carbon nanotube reinforced composite using FSDT and Donnell's kinematic assumptions. Additionally, a considerable number of research articles are reported on the advanced composite structure by modifying the available kinematic theories to reduce the total number of unknowns for the mathematical simplicity (Belabed *et al.* 2018, Mokhtar *et al.* 2018, Mouffoki *et al.* 2017) and the solution techniques (Mehrparvar and Ghannadpour 2018, Ovesy *et al.* 2015, Sherafat and Ovesy 2013, Ghannadpour *et al.* 2012a, Ghannadpour *et al*. 2012b) including the geometrical large deformation behavior (Ovesy and Ghannadpour 2007, Ghannadpour and Alinia 2006, Alinia and Ghannadpour 2009, Ghannadpour *et al.* 2012).

The previously published articles related to the analysis of eigenfrequency responses via the higher-order polynomial displacement kinematics for the FG curved panel under thermal environment including the temperature-dependent properties are very few in numbers. However, this is the first time attempted by the authors to compute the free vibration frequency values of the heated shear deformable FG tilted panel under different thermal field (uniform and linear temperature rise). Additionally, the proposed model is derived in rectangular and tilted planforms to achieve the required form. Similarly, the model is also capable of constructing various shell configurations (flat, spherical, elliptical cylindrical and hyperbolic) with the help of variable curvature ratio. For the computational solution purpose, a linear finite element model is derived for the tilted FG structure in the framework of the third-order shear deformation kinematic theory (TSDT). The necessary frequency solutions are worked out via a home-made suitable MATLAB code in conjunction with higher-order FG model including the temperature effect. The proposed and derived numerical model validity is verified by solving the adequate numbers of numerical examples related to the convergence including the corresponding comparison behaviour. Finally, the model is extended to explore the influences of the geometrical parameters (thickness ratios, shallowness ratios, power-law indices, aspect ratios) on the eigenfrequencies of the tilted FG including the variable thermal fields and temperature dependent elastic properties are illustrated in details.

2. Effective material properties of FGM

In general, the structural properties affect considerably due to the elevated thermal environment and incurred in the structural modelling with the help of modified steps (Attia *et al.* 2018, Karami *et al.* 2018, Menasria *et al.* 2017, Chikh *et al.* 2017, El-Haina *et al.* 2017, Bousahla *et al.* 2016, Bouderba *et al.* 2016, Beldjelili *et al.* 2016). The current FGM panel contains smoothly graded metal and ceramic material from lower (metal-rich) to upper (ceramic-rich) surfaces. The elastic properties of the individual constituents are considered to be temperature-dependent and included in the current modelling via the following expression as (Reddy and Chin 1998)

$$\chi_{c,m}(T) = \chi_0(\chi_{-1}T^{-1} + 1 + \chi_1 T + \chi_2 T^2 + \chi_3 T^3) \tag{1}$$

where, χ_c and χ_m are the effective elastic properties of the ceramic and the metal fractions, respectively, whereas χ_0, χ_{-1}, χ_1, χ_2 and χ_3 are the corresponding temperature coefficients.

Further, to achieve the necessary material grading through the spatial direction (z), the power-law distribution of volume fractions of FGM constituents are adopted, as (Shen 2009)

$$\vartheta_c(z) = \left(\frac{z}{h?} + \frac{1}{\ }\right)^n \quad \text{and}$$

$$\vartheta_m(z) = 1 - \vartheta_c(z) \qquad \begin{cases} 0 \le n \to \infty \\ -\dfrac{h}{2} \le z \le \dfrac{h}{2} \end{cases} \tag{2}$$

where, ϑ_m and ϑ_c are the volume fractions of the metal and the ceramic, respectively. Here, n represents the power-law index and which decides the material profile across the spatial direction.

Therefore, the overall material properties of FGM are functions of temperature and spatial coordinate. The overall material properties for FGM (χ) are obtained using the generalized Voigt's material model (Gibson *et al.* 1995)

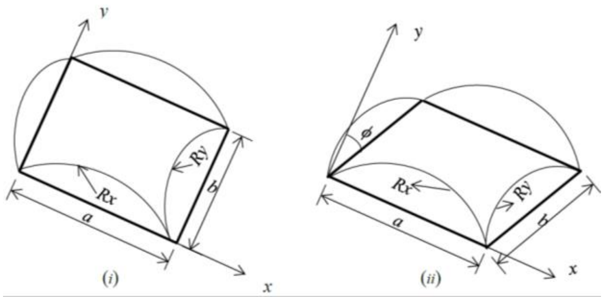

Fig. 1 FG shallow shell structure in two different planforms (*i*) rectangle form (*ii*) tilted form

$$\chi(T,z)=\chi_c(T)\vartheta_c(z)+\chi_m(T)\vartheta_m(z) \tag{3}$$

3. Mathematical formulations

3.1 Mid-plane kinematics

A general shallow shell panel structure of sides *a* and *b*, and thickness *h*, is employed in two different planforms (rectangular and tilted) as shown in Fig. 1. Here, R_x and R_y are the radii of curvature along x and y direction, respectively. Also, different geometrical configuration (Karami *et al.* 2018, Karami *et al.* 2018, Zine *et al.* 2018) plays a critical role in the structural analysis and design. The structural kinematics has been modelled every now and then via different types kinematic theories including the modified version of polynomial based displacement function to approximate the deformation behaviour (Fourn *et al.* 2018, Yazid *et al.* 2018, Abdelaziz *et al.* 2017, Bellifa *et al.* 2017, Bellifa *et al.* 2016). However, in this current study a TSDT mid-plane kinematics model is utilized to define the global displacements (u, v, w) at any point in terms of mid-plane displacements (u_0, v_0, w_0), rotations (θ_x, θ_y) and higher-order ($u_0^*, v_0^*, \theta_x^*, \theta_y^*$) terms without considering the mid-plane stretching effect (Benchohra *et al.* 2018, Abualnour *et al.* 2018, Younsi *et al.* 2018, Bouhadra *et al.* 2018), as (Reddy 2004)

$$\left.\begin{aligned} u &= u_0 + z\theta_x + z^2 u_0^* + z^3\theta_x^* \\ v &= v_0 + z\theta_y + z^2 v_0^* + z^3\theta_y^* \\ w &= w_0 \end{aligned}\right\} \tag{4}$$

This kinematic model can be again rewritten in the matrix form as

$$\{\delta\}=[f]\{\delta_0\} \tag{5}$$

where, $\{\delta\}=\lfloor u \quad v \quad w \rfloor^T$ and $\{\delta_0\}=\lfloor u_0 \quad v_0 \quad w_0 \quad \theta_x \quad \theta_y \quad u_0^* \quad v_0^* \quad \theta_x^* \quad \theta_y^* \rfloor^T$ are the global and mid-plane displacement vectors. $[f]$ contains the thickness coordinate functions as expressed here.

$$[f]=\begin{bmatrix} 1 & 0 & 0 & z & 0 & z^2 & 0 & z^3 & 0 \\ 0 & 1 & 0 & 0 & z & 0 & z^2 & 0 & z^3 \\ 0 & 0 & 1 & 0 & 0 & 0 & 0 & 0 & 0 \end{bmatrix} \tag{6}$$

The rectangular and tilted (tilted angle ϕ with respect to *y*-axis) planforms are shown in Fig. 1 with sides *a* and *b*. To constraint the oblique edges, the local displacement vector is required to transform to global via transformation matrix [*H*] which comprises cosine (*l*) and sine (*m*) terms. The displacement transformation can be expressed as

$$\begin{Bmatrix} u_0 \\ v_0 \\ w_0 \\ \theta_x \\ \theta_y \\ u_0^* \\ v_0^* \\ \theta_x^* \\ \theta_y^* \end{Bmatrix}=\begin{bmatrix} l & -m & 0 & 0 & 0 & 0 & 0 & 0 & 0 \\ m & l & 0 & 0 & 0 & 0 & 0 & 0 & 0 \\ 0 & 0 & 1 & 0 & 0 & 0 & 0 & 0 & 0 \\ 0 & 0 & 0 & l & -m & 0 & 0 & 0 & 0 \\ 0 & 0 & 0 & m & l & 0 & 0 & 0 & 0 \\ 0 & 0 & 0 & 0 & 0 & l & -m & 0 & 0 \\ 0 & 0 & 0 & 0 & 0 & m & l & 0 & 0 \\ 0 & 0 & 0 & 0 & 0 & 0 & 0 & l & -m \\ 0 & 0 & 0 & 0 & 0 & 0 & 0 & m & l \end{bmatrix}\begin{Bmatrix} u_0' \\ v_0' \\ w_0' \\ \theta_x' \\ \theta_y' \\ u_0^{*'} \\ v_0^{*'} \\ \theta_x^{*'} \\ \theta_y^{*'} \end{Bmatrix} \tag{7}$$

Eq. (7) can also be written as

$$\{\delta_0\}=[H]\{\delta_0'\} \tag{8}$$

where, $\{\delta_0'\}$ is the displacement field defined in the local coordinates.

The strain-displacement equation for any general shallow shell structure can be written as

$$\begin{Bmatrix} \varepsilon_{xx} \\ \varepsilon_{yy} \\ \gamma_{xy} \\ \gamma_{xz} \\ \gamma_{yz} \end{Bmatrix}=\left\{\left(\frac{\partial u}{\partial x}+\frac{w}{R_x}\right) \; \left(\frac{\partial v}{\partial y}+\frac{w}{R_y}\right) \; \left(\frac{\partial u}{\partial y}+\frac{\partial v}{\partial x}\right) \; \left(\frac{\partial u}{\partial z}+\frac{\partial w}{\partial x}-\frac{u}{R_x}\right) \; \left(\frac{\partial v}{\partial z}+\frac{\partial w}{\partial y}-\frac{v}{R_y}\right)\right\}^T \tag{9}$$

By imposing the displacement terms (4) in the strain-displacement Eq. (9), the global strain tensor can be modified as

$$\begin{Bmatrix} \varepsilon_{xx} \\ \varepsilon_{yy} \\ \gamma_{xy} \\ \gamma_{xz} \\ \gamma_{yz} \end{Bmatrix}=\begin{Bmatrix} \varepsilon_x^{\ 0} \\ \varepsilon_y^{\ 0} \\ \varepsilon_{xy}^{\ 0} \\ \varepsilon_{xz}^{\ 0} \\ \varepsilon_{yz}^{\ 0} \end{Bmatrix}+z\begin{Bmatrix} k_x^{\ 1} \\ k_y^{\ 1} \\ k_{xy}^{\ 1} \\ k_{xz}^{\ 1} \\ k_{yz}^{\ 1} \end{Bmatrix}+z^2\begin{Bmatrix} k_x^{\ 2} \\ k_y^{\ 2} \\ k_{xy}^{\ 2} \\ k_{xz}^{\ 2} \\ k_{yz}^{\ 2} \end{Bmatrix}+z^3\begin{Bmatrix} k_x^{\ 3} \\ k_y^{\ 3} \\ k_{xy}^{\ 3} \\ k_{xz}^{\ 3} \\ k_{yz}^{\ 3} \end{Bmatrix} \tag{10}$$

$$\varepsilon=\varepsilon^0+zk^1+z^2k^2+z^3k^3 \tag{11}$$

where, ε^0, k^1, k^2 and k^3 are the mid-plane strain, curvature and higher-order terms, respectively and presented in Kar and Panda (2015).

Eq. (11) can be again rearranged as

$$\{\varepsilon\}=[T]\{\bar{\varepsilon}\} \tag{12}$$

where, $\{\bar{\varepsilon}\}=\lfloor \varepsilon^0 \quad k^1 \quad k^2 \quad k^3 \rfloor^T$ is the mid-plane strain, and $T = \begin{bmatrix} I & zI & z^2 I & z^3 I \end{bmatrix}$ is the thickness-coordinate matrix, in which I is the unit matrix of size 5×5.

3.2 Constitutive equations

The stress-strain equation for the FG shallow shell structure is given by

$$\begin{Bmatrix} \sigma_{xx} \\ \sigma_{yy} \\ \tau_{xy} \\ \tau_{xz} \\ \tau_{yz} \end{Bmatrix} = \begin{bmatrix} \frac{E}{1-v^2} & \frac{vE}{1-v^2} & 0 & 0 & 0 \\ \frac{vE}{1-v^2} & \frac{E}{1-v^2} & 0 & 0 & 0 \\ 0 & 0 & \frac{E}{2(1+v)} & 0 & 0 \\ 0 & 0 & 0 & \frac{E}{2(1+v)} & 0 \\ 0 & 0 & 0 & 0 & \frac{E}{2(1+v)} \end{bmatrix} \left(\begin{Bmatrix} \varepsilon_{xx} \\ \varepsilon_{yy} \\ \gamma_{xy} \\ \gamma_{xz} \\ \gamma_{yz} \end{Bmatrix} - \begin{bmatrix} 1 \\ 1 \\ 0 \\ 0 \\ 0 \end{bmatrix} \alpha \Delta T \right) \tag{13}$$

Eq. (13) can also be written as

$$\{\sigma\} = [Q]\left(\{\varepsilon\} - \{\varepsilon_{th}\}\right) \tag{14}$$

where, $[Q]$ and $\{\varepsilon_{th}\}$ are the material matrix and the thermal strain.

The strain energy of the FG shallow shell structure can be presented as

$$U = \frac{1}{2}\iint \left(\int_{-h/2}^{+h/2} \{\varepsilon\}^T [Q]\{\varepsilon\}\, dz \right) dxdy \tag{15}$$

By imposing Eq. (12) in Eq. (15), the strain energy can be modified as

$$U = \frac{1}{2}\iint \left(\{\varepsilon\}^T [D]\{\varepsilon\} \right) dxdy \tag{16}$$

where, $[D] = \int_{-h/2}^{+h/2} [T]^T [Q][T]\, dz$ is the rigidity matrix.

The membrane strain energy due to the temperature rise through the spatial direction of FG shallow shell structure can be written in Green-Lagrange sense, as (Cook *et al.* 2009)

$$U_m = \int_v \begin{bmatrix} \frac{1}{2}\left\{(u,_x)^2 + (v,_x)^2 + (w,_x)^2\right\} N_x + \frac{1}{2}\left\{(u,_y)^2 + (v,_y)^2 + (w,_y)^2\right\} N_y \\ + \left\{u,_x u,_y + v,_x v,_y + w,_x w,_y\right\} N_{xy} \end{bmatrix} dv \tag{17}$$

where, N_x, N_y and N_{xy} are the thermal force resultants.

$$U_m = \frac{1}{2}\iint \left[\{\bar{\varepsilon}_G\}^T [D_G]\{\bar{\varepsilon}_G\} \right] dxdy \tag{18}$$

where, $[D_G]$ and $\{\bar{\varepsilon}_G\}$ denote the material property matrix and the geometrical mid-plane strain, respectively.

The total kinetic energy of the FG shallow shell structure can be written as

$$T = \frac{1}{2}\int_V \rho \{\dot{\delta}\}^T \{\dot{\delta}\}\, dV \tag{19}$$

where, $\{\dot{\delta}\}$ and ρ represent the global velocity vector and the mass density, respectively.

Now, by imposing Eq. (5) in Eq. (19), the total kinetic energy of the FG shallow shell structure can be modified and expressed as

$$T = \frac{1}{2}\int_A \{\dot{\delta}_0\}^T [m]\{\dot{\delta}_0\}\, dA \tag{20}$$

where, $[m] = \int_{-h/2}^{+h/2} [f]^T \rho [f]\, dz$ denotes the inertia matrix.

3.3 Finite element approximations

In this section, the present FG shallow shell panel in rectangular/tilted planform is discretized using a nine-noded element with eighty-one degrees-of-freedom. The displacements defined in the mid-plane can be written in nodal form as

$$\{\delta_0\} = \sum_{i=1}^{9} N_i \{\delta_{0_i}\} \tag{21}$$

where, $\{\delta_{0_i}\}$ and N_i are the nodal displacement vector and the approximation function at i^{th} node (Cook *et al.* 2009).

Now, the total and geometric mid-plane strain vectors can be expressed using Eq. (21) as

$$\{\bar{\varepsilon}\} = [B]\{\delta_{0_i}\} \text{ and } \{\bar{\varepsilon}_G\} = [B_G]\{\delta_{0_i}\} \tag{22}$$

where, $[B]$ and $[B_G]$ are the differential operators of the total and geometrical mid-plane strains, respectively.

To obtain the governing equation of the thermally vibrated FG shallow shell structure, Hamilton's principle is employed, as

$$\delta \int_{t_1}^{t_2} (T - (U + U_m))\, dt = 0 \tag{23}$$

By imposing Eqs. (16)-(22) in the above governing equation, the equilibrium equation of the thermally vibrated FG shallow shell structure is achieved and expressed in global form, as

$$\left([K] - [K_G] - \omega^2 [M]\right)\Delta = 0 \tag{24}$$

where, $[M] = [N]^T [m][N]$ is the global mass matrix, $[K] = [B]^T [D][B]$ is the global stiffness matrix, $[K_G] = [B_G]^T [D_G][B_G]$ is the geometric stiffness matrix and ω and Δ are the eigenvalues and the corresponding eigenvectors, respectively.

4. Results and discussion

The thermoelastic eigenfrequency responses of the simply supported rectangular/tilted FG shallow shell panel

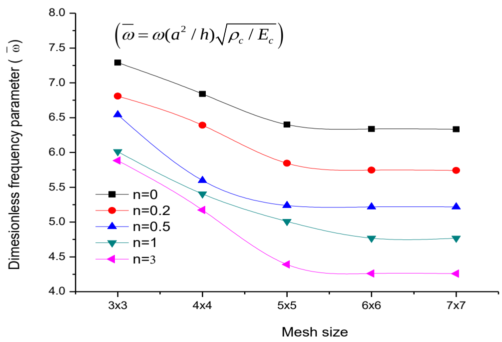

Fig. 2 Dimensionless frequency parameters of a simply-supported tilted FG panel

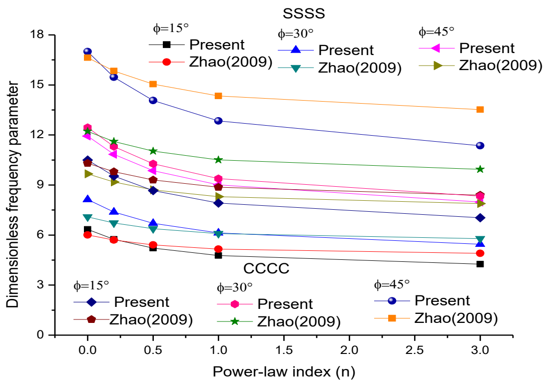

Fig. 3 Dimensionless frequency parameters of tilted FG panels under simply supported and clamped support conditions

structures are obtained under the influence of variable thermal field (uniform and linear temperature rise). For the computational purpose, a suitable computer algorithm has been prepared (MATLAB environment) using the proposed higher-order finite element formulations. Firstly, the convergence and subsequent model validity are performed to display model accuracy. Later, the frequency responses of FG rectangle/tilted panels are explored via solving different numerical examples with the help of the currently derived higher-order finite element model.

4.1 Convergence and comparison study

Firstly, the model engaged to comply with the steadiness of the numerical solution by varying the mesh densities. Hence, an example problem of simply supported FG (Al/ZrO_2) tilted (θ=30°) panel (a/h=10) is carried out. The computed dimensionless frequency parameters $\left(\overline{\omega}=\omega(a^2/h)\sqrt{\rho_c/E_c}\right)$ versus the power-law indices (n = 0, 0.2, 0.5, 2, 3) for the different mesh divisions are provided in Fig. 2. From the figure, it is understood that the frequency responses of the FG tilted panels following good convergence rate with the element densities and a (6×6), mesh sufficient for the evaluation of new results.

To display the correctness of the FE based frequency solution of the FG panel structure, the results are obtained and compared with the published data. Fig. 3 exhibits the dimensionless frequencies of the tilted (θ=15°, 30°, 45°) FG panels for two types of end constraints (clamped and simply support). The present results are closely aligned with the reported results of the source (Zhao 2009) almost every case. However, the reported results of the source (Zhao 2009) are evaluated using the FSDT type of displacement kinematics, hence, the reference values are comparatively higher than the derived TSDT results.

4.2 Numerical examples

The influences of various parameters of rectangular

Table 1 Temperature-dependent properties of the FGM constituents (Huang and Shen 2004)

Materials	Properties	χ_0	χ_{-1}	χ_1	χ_2	χ_3
ZrO_2	E (Pa)	2.4427×10^{11}	0	-1.3710×10^{-3}	1.2140×10^{-6}	-3.6810×10^{-10}
	A (K^{-1})	12.766×10^{-6}	0	-1.4910×10^{-3}	1.0060×10^{-5}	-6.7780×10^{-11}
Ti-6Al-4V	E (Pa)	1.2256×10^{11}	0	-4.5860×10^{-4}	0	0
	α (K^{-1})	7.5788×10^{-6}	0	6.6380×10^{-4}	-3.1470×10^{-6}	0

Table 2 Influence of power-law index on the dimensionless frequency parameters of FG rectangular and tilted flat/curved panels under uniform and linear temperature rise

Shell Configurations	T (K)	Uniform temperature rise				Linear temperature rise			
		n=0.5		n=5		n=0.5		n=5	
		ϕ = 0°	ϕ = 30°	ϕ = 0°	ϕ = 30°	ϕ = 0°	ϕ = 30°	ϕ = 0°	ϕ = 30°
Flat (R_x=R_y=∞)	300	7.554	14.743	6.350	12.362	7.554	14.743	6.350	12.362
	400	7.232	14.120	6.127	11.939	7.363	14.389	6.211	12.110
	500	6.961	13.594	5.925	11.549	7.202	14.085	6.091	11.887
	600	6.738	13.158	5.740	11.190	7.070	13.831	5.988	11.693
	700	6.556	12.802	5.571	10.857	6.965	13.625	5.902	11.527
Spherical (R_x=R_y=R)	300	32.035	36.742	26.294	30.305	32.035	36.742	26.294	30.305
	400	30.635	35.152	25.404	29.282	31.187	35.803	25.733	29.676
	500	29.467	33.821	24.582	28.334	30.457	34.995	25.233	29.115
	600	28.516	32.732	23.819	27.455	29.842	34.315	24.789	28.620
	700	27.761	31.859	23.107	26.634	29.335	33.755	24.397	28.184
Cylindrical (R_x=R, R_y=∞)	300	20.690	26.043	17.298	21.334	20.690	26.043	17.298	21.334
	400	19.811	24.915	16.707	20.627	20.185	25.391	16.943	20.910
	500	19.070	23.971	16.162	19.967	19.752	24.829	16.629	20.529
	600	18.458	23.199	15.659	19.349	19.391	24.352	16.355	20.190
	700	17.961	22.581	15.194	18.766	19.097	23.956	16.118	19.888
Hyperbolic (R_x=R, R=-R_y)	300	29.782	31.119	24.166	25.364	29.782	31.119	24.166	25.364
	400	28.489	29.788	23.386	24.554	29.054	30.411	23.714	24.922
	500	27.407	28.669	22.649	23.786	28.422	29.795	23.304	24.521
	600	26.524	27.748	21.951	23.053	27.881	29.266	22.931	24.157
	700	25.819	27.003	21.283	22.349	27.424	28.820	22.594	23.829
Elliptical (R_x=R, R_y=2R)	300	24.328	30.297	20.172	24.753	24.328	30.297	20.172	24.753
	400	23.274	28.972	19.478	23.927	23.687	29.507	19.733	24.241
	500	22.391	27.867	18.841	23.158	23.138	28.825	19.353	23.781
	600	21.670	26.968	18.255	22.441	22.679	28.249	19.002	23.371
	700	21.093	26.254	17.713	21.767	22.304	27.769	18.705	23.006

Table 3 Influence of thickness ratio on the dimensionless frequency parameters of FG rectangular and tilted flat/curved panels under uniform and linear temperature rise

Shell Configurations	T (K)	Uniform temperature rise				Linear temperature rise			
		a/h=10		a/h=50		a/h=10		a/h=50	
		$\phi=0°$	$\phi=30°$	$\phi=0°$	$\phi=30°$	$\phi=0°$	$\phi=30°$	$\phi=0°$	$\phi=30°$
Flat (R_x=R_y=∞)	300	6.440	9.030	6.699	12.304	6.440	9.030	6.699	12.304
	400	6.200	8.699	6.448	11.856	6.289	8.830	6.539	12.037
	500	5.987	8.403	6.226	11.454	6.159	8.657	6.404	11.804
	600	5.798	8.140	6.030	11.095	6.051	8.509	6.291	11.606
	700	5.632	7.904	5.857	10.773	5.960	8.386	6.200	11.441
Spherical (R_x=R_y=R)	300	7.466	9.701	18.018	19.739	7.466	9.701	18.018	19.739
	400	7.165	9.328	17.319	18.991	7.243	9.449	17.539	19.250
	500	6.905	9.000	16.708	18.331	7.052	9.232	17.121	18.823
	600	6.685	8.716	16.180	17.753	6.892	9.048	16.761	18.458
	700	6.500	8.469	15.723	17.247	6.762	8.895	16.456	17.148
Cylindrical (R_x=R, R_y=∞)	300	6.897	9.319	12.656	15.619	6.897	9.319	12.656	15.619
	400	6.627	8.970	12.157	15.041	6.708	9.096	12.304	15.260
	500	6.392	8.660	11.724	14.525	6.547	8.903	11.999	14.947
	600	6.189	8.387	11.353	14.069	6.413	8.740	11.739	14.679
	700	6.016	8.147	11.035	13.664	6.303	8.603	11.521	14.453
Hyperbolic (R_x=R, R=-R_y)	300	6.910	9.324	14.294	17.076	6.910	9.324	14.294	17.076
	400	6.653	8.986	13.771	16.473	6.749	9.123	13.980	16.744
	500	6.424	8.682	13.303	15.925	6.611	8.950	13.705	16.452
	600	6.222	8.410	12.886	15.428	6.496	8.801	13.466	16.197
	700	6.043	8.165	12.513	14.975	6.400	8.676	13.261	15.978
Elliptical (R_x=R, R_y=$2R$)	300	7.115	9.464	14.746	17.119	7.115	9.464	14.746	17.119
	400	6.831	9.104	14.163	16.473	6.909	9.227	14.332	16.701
	500	6.586	8.787	13.658	15.902	6.734	9.022	13.974	16.337
	600	6.376	8.510	13.225	15.401	6.587	8.849	13.667	16.026
	700	6.199	8.268	12.855	14.961	6.468	8.705	13.408	15.764

Table 4 Influence of aspect ratio on the dimensionless frequency parameters of FG rectangular and tilted flat/curved panels under uniform and linear temperature rise

Shell Configurations	T(K)	Uniform temperature rise				Linear temperature rise			
		a/b=1		a/b=3		a/b=1		a/b=3	
		$\phi=0°$	$\phi=30°$	$\phi=0°$	$\phi=30°$	$\phi=0°$	$\phi=30°$	$\phi=0°$	$\phi=30°$
Flat (R_x=R_y=∞)	300	6.713	13.053	33.577	45.545	6.713	13.053	33.577	45.545
	400	6.462	12.577	32.312	43.837	6.553	12.767	32.762	44.456
	500	6.239	12.150	31.193	42.325	6.417	12.519	32.073	43.532
	600	6.042	11.769	30.211	40.992	6.304	12.309	31.503	42.765
	700	5.869	11.428	29.347	39.818	6.212	12.135	31.040	42.140
Spherical (R_x=R_y=R)	300	28.125	32.302	48.787	57.442	28.125	32.302	48.787	57.442
	400	27.069	31.104	46.787	55.101	27.450	31.556	47.266	55.681
	500	26.135	30.038	45.076	55.095	26.863	30.906	45.962	54.179
	600	25.312	29.093	43.638	51.402	26.360	30.349	44.867	52.923
	700	24.587	28.256	42.440	49.987	25.933	29.879	43.963	51.893
Cylindrical (R_x=R, R_y=∞)	300	18.297	22.799	40.070	49.988	18.297	22.799	40.070	49.988
	400	17.627	21.959	38.519	48.081	17.890	22.285	39.013	48.725
	500	17.027	21.210	37.164	46.403	17.538	21.837	38.112	47.650
	600	16.492	20.544	35.988	44.939	17.239	21.450	37.357	46.753
	700	16.015	19.951	34.972	43.661	16.991	21.120	36.736	46.018
Hyperbolic (R_x=R, R=-R_y)	300	25.914	27.084	40.828	50.331	25.914	27.084	40.828	50.331
	400	24.971	26.119	39.440	48.615	25.355	26.542	40.149	49.481
	500	24.126	25.246	38.159	47.032	24.861	26.063	39.557	48.744
	600	23.369	24.457	36.974	45.571	24.430	25.644	39.046	48.114
	700	22.691	23.741	35.871	44.213	24.055	25.281	38.609	47.580
Elliptical (R_x=R, R_y=$2R$)	300	21.472	26.520	43.468	52.871	21.472	26.520	43.468	52.871
	400	20.666	25.531	41.716	50.786	20.956	25.897	42.175	51.358
	500	19.952	24.653	40.208	48.949	20.509	25.353	41.071	50.070
	600	19.324	23.877	38.928	47.394	20.129	24.883	40.146	48.996
	700	18.771	23.192	37.851	46.074	19.812	24.483	39.386	48.118

tilted FG flat and curved panels subjected to uniform and linear thermal field on the frequency responses are examined and discussed here. Various shell configurations such as flat (R_x=R_y=∞), singly-curved (cylindrical: R_x=R and R_y=∞), doubly-curved (hyperbolic: R_x=R, R_y=-R, spherical: R_x=R_y=R, elliptical: R_x=R, R_y=$2R$) in rectangular and tilted planform are considered throughout the investigations. Titanium alloy (*Ti*-6*Al-4V)* and zirconia (ZrO_2) are considered as FGM constituents, and the temperature-dependent properties are mentioned in Table 1. However, the Poisson's ratios (υ) and densities (ρ) are presumed to temperature-independent and taken as 0.3 (for both materials), 3000 kg/m^3 (for ZrO_2) and 4427 kg/m^3 (for *Ti*-6*Al*-4*V*). The dimensionless frequency parameters ($\overline{\omega}=\omega(a^2/h)\sqrt{(1-v_m^2)\rho_m/E_0}$), where, E_0 represents the Young's modulus of metal at ambient temperature, are computed for different set of parameters by varying shallowness ratio (R/a), thickness ratio (a/h), aspect ratio (a/b), power-law index (n) and temperature variations (uniform and linear).

Example 1: Table 2 demonstrates the eigenfrequency responses of FG (*Ti*-6*Al*-4*V*/ZrO_2) panels (R/a=5, a/h=100 and a/b=1) for two different power-law indices (n = 0.5 and 5) under uniform and linear temperature rise (300 K to 700 K). The results predict that ceramic-rich (n=0.5) FG panels have higher frequency parameters than the metal-rich (n=5) FG panels, because ceramic-rich FG panels are stiffer than the metal-rich.

Example 2: Table 3 demonstrates the eigenfrequency responses of FG (*Ti*-6*Al-4V*/ZrO_2) rectangular/tilted panels (R/a=5, n=2 and a/b=1) for different thickness ratios (a/h=10 and 50) under uniform and linear temperature rise. The frequency parameters are enhancing with the thickness ratios i.e., thin (a/h=50) FG panels have comparatively higher frequency parameters than the moderately thick (a/h=10) FG panels, in all the cases considered here.

Example 3: Table 4 demonstrates the eigenfrequency responses of FG (*Ti*-6*Al-4V*/ZrO_2) rectangular/tilted panels (R/a=5, n=2 and a/h=100) for two aspect ratios (a/b=1 and

Table 5 Influence of shallowness ratio on the dimensionless frequency parameters of FG rectangular and tilted curved panels under uniform and linear temperature rise

Shell Configurations	T(K)	Uniform temperature rise				Linear temperature rise			
		R/a=5		R/a=20		R/a=5		R/a=20	
		ϕ = 0°	ϕ = 30°	ϕ = 0°	ϕ = 30°	ϕ = 0°	ϕ = 30°	ϕ = 0°	ϕ = 30°
Spherical (R_x=R_y=R)	300	28.125	32.302	11.043	15.241	28.125	32.302	11.043	15.241
	400	27.069	31.104	10.594	14.667	27.450	31.556	10.706	14.870
	500	26.135	30.038	10.208	14.159	26.863	30.906	10.415	14.550
	600	25.312	29.093	9.883	13.713	26.360	30.349	10.170	14.278
	700	24.587	28.256	9.611	13.321	25.933	29.879	9.966	14.051
Cylindrical (R_x=R, R_y=∞)	300	18.297	22.799	8.772	13.907	18.297	22.799	8.772	13.907
	400	17.627	21.959	8.419	13.396	17.890	22.285	8.512	13.596
	500	17.027	21.210	8.115	12.940	17.538	21.837	8.290	13.325
	600	16.492	20.544	7.856	12.533	17.239	21.450	8.103	13.096
	700	16.015	19.951	7.639	12.171	16.991	21.120	7.950	12.906
Hyperbolic (R_x=R, R=-R_y)	300	25.914	27.084	9.226	14.246	25.914	27.084	9.226	14.246
	400	24.971	26.119	8.886	13.740	25.355	26.542	9.017	13.961
	500	24.126	25.246	8.582	13.280	24.861	26.063	8.835	13.712
	600	23.369	24.457	8.312	12.865	24.430	25.644	8.681	13.499
	700	22.691	23.741	8.073	12.489	24.055	25.281	8.551	13.320
Elliptical (R_x=R, R_y=2R)	300	21.472	26.520	9.638	14.381	21.472	26.520	9.638	14.381
	400	20.666	25.531	9.244	13.846	20.956	25.897	9.340	14.043
	500	19.952	24.653	8.907	13.369	20.509	25.353	9.084	13.751
	600	19.324	23.877	8.622	12.948	20.129	24.883	8.869	13.502
	700	18.771	23.192	8.385	12.577	19.812	24.483	8.692	13.296

3). The frequency parameters are following an accelerating path while the aspect ratio increase i.e., a/b=3 irrespective of the geometrical configuration and temperature loading.

Example 4: Table 5 shows the eigenfrequency responses of FG (Ti-6Al-4V/ZrO_2) rectangular/tilted panels (a/b=1, n=2 and a/h=100) for different panel shallowness ratios (R/a=5 and 20) under the two temperature loading (uniform and linear). The FG panels with small shallowness values exhibit the higher frequency parameters due to their high membrane strength in comparison to the higher one.

Example 5: The tilted FG panels (ϕ=30°) are demonstrating higher frequency parameters than the rectangular panels (ϕ=0°), irrespective of geometrical configuration and input parameter. Hence, the frequency responses are gradually enhancing with the tilt angle from ϕ=0° to ϕ=45° (refer Table 6). This is because the tilted panels are stiffer than the rectangular one. The FG panels subjected to linear temperature variation have higher frequency parameters, compared to the uniform temperature field, and the responses are continually deteriorating with the temperature rise. The spherical FG panels, both in rectangular and tilted form, are exhibiting maximum frequency parameter, whereas minimum for flat FG panels.

5. Conclusions

In this investigation, the eigenvalue characteristics of

Table 6 Influence of tilt angle on the dimensionless frequency parameters of FG flat/curved panels under uniform and linear temperature rise

Shell Configurations	$T(K)$	Uniform temperature rise					Linear temperature rise				
		ϕ =0°	ϕ =15°	ϕ = 22.5°	ϕ =30°	ϕ =45°	ϕ = 0°	ϕ =15°	ϕ = 22.5°	ϕ =30°	ϕ =45°
Flat (R_x=R_y=∞)	300	6.713	10.235	11.431	13.053	19.452	6.713	10.235	11.431	13.053	19.452
	400	6.462	9.862	11.014	12.577	18.744	6.553	10.012	11.180	12.767	19.028
	500	6.239	9.527	10.640	12.150	18.107	6.417	9.817	10.963	12.519	18.659
	600	6.042	9.229	10.306	11.769	17.539	6.304	9.653	10.779	12.309	18.346
	700	5.869	8.961	10.007	11.428	17.031	6.212	9.516	10.627	12.135	18.088
Spherical (R_x=R_y=R)	300	28.125	29.607	30.649	32.302	34.996	28.125	29.607	30.649	32.302	34.996
	400	27.069	28.507	29.512	31.104	33.687	27.450	28.921	29.941	31.556	34.166
	500	26.135	27.530	28.500	30.038	32.526	26.863	28.323	29.324	30.906	33.442
	600	25.312	26.664	27.604	29.093	31.503	26.360	27.810	28.794	30.349	32.819
	700	24.587	25.897	26.810	28.256	30.599	25.933	27.374	28.346	29.879	32.288
Cylindrical (R_x=R, R_y=∞)	300	18.297	21.681	22.042	22.799	27.032	18.297	21.681	22.042	22.799	27.032
	400	17.627	20.880	21.229	21.959	26.038	17.890	21.189	21.544	22.285	26.426
	500	17.027	20.167	20.504	21.210	25.150	17.538	20.758	21.108	21.837	25.898
	600	16.492	19.534	19.860	20.544	24.361	17.239	20.386	20.732	21.450	25.444
	700	16.015	18.970	19.287	19.951	23.657	16.991	20.068	20.411	21.120	25.060
Hyperbolic (R_x=R, R=-R_y)	300	25.914	26.289	26.568	27.084	30.175	25.914	26.289	26.568	27.084	30.175
	400	24.971	25.346	25.618	26.119	29.101	25.355	25.750	26.030	26.542	29.571
	500	24.126	24.495	24.761	25.246	28.128	24.861	25.274	25.555	26.063	29.040
	600	23.369	23.729	23.987	24.457	27.249	24.430	24.858	25.140	25.644	28.578
	700	22.691	23.036	23.285	23.741	26.451	24.055	24.496	24.779	25.281	28.181
Elliptical (R_x=R, R_y=2R)	300	21.472	25.821	26.017	26.520	29.917	21.472	25.821	26.017	26.520	29.917
	400	20.666	24.861	25.047	25.531	28.802	20.956	25.220	25.408	25.897	29.215
	500	19.952	24.007	24.187	24.653	27.811	20.509	24.694	24.876	25.353	28.603
	600	19.324	23.252	23.426	23.877	26.936	20.129	24.238	24.416	24.883	28.077
	700	18.771	22.584	22.753	23.192	26.163	19.812	23.848	24.022	24.483	27.632

FG shallow shell panel structures in both, rectangular and tilted forms are investigated under uniform and linear thermal fields including temperature-dependent elastic properties. The final effective properties of the FG structure are computed using Voigt's model in the framework of the power-law including the effect of temperature dependency. The eigenvalue equation of the vibrating heated FG (rectangular/tilted) shallow shell structure is governed through the generalized Hamilton's principle. The 2D approximated finite element solutions for the present FG model are obtained using Lagrangian isoparametric Q9 element. Finally, the dimensionless frequency parameters of the simply supported heated FG shallow shell panel structures are examined with both the rectangular and tilted planforms for different geometry (thickness, aspect and shallowness ratios), grading (power-law indices) and temperature field (uniform and linear temperature rise) related parameters. Based on the comprehensive parametric investigation, the following significant inferences are furnished in the following lines.

• The ceramic-rich tilted FG shallow shell structures demonstrate larger frequency parameters compared to the metal-rich FGM.

• The frequency parameters of rectangular/tilted FG shallow shell panel structures are following an increasing trend while the aspect ratio values increase for each type of geometrical configurations.

• The frequency responses are higher while the skew angle increases, irrespective of geometry, material profile and temperature variation. In addition, the spherical and flat the FG panels demonstrate maximum and minimum frequency parameters, respectively, in both the rectangular or tilted forms.

• The frequency responses follow deteriorating type of behaviour with the enhancement in temperature values. However, the rectangular/tilted FG panels subjected to linear temperature field exemplify higher frequency parameters while compared to the uniform temperature field.

References

Abdelaziz, H.H., Meziane, M.A.A., Bousahla, A.A., Tounsi, A., Mahmoud, S.R. and Alwabli, A.S. (2017), "An efficient hyperbolic shear deformation theory for bending, buckling and free vibration of FGM sandwich plates with various boundary conditions", *Steel Compos. Struct.*, **25**(6), 693-704.

Abualnour, M., Houari, M.S.A., Tounsi, A. and Mahmoud, S.R. (2018), "A novel quasi-3D trigonometric plate theory for free vibration analysis of advanced composite plates", *Compos. Struct.*, **184**, 688-697.

Alinia, M.M. and Ghannadpour, S.A.M. (2009), "Nonlinear analysis of pressure loaded FGM plates", *Compos. Struct.*, **88**(3), 354-359.

Amnieh, H.B., Zamzam, M.S. and Kolahchi, R. (2018), "Dynamic analysis of non-homogeneous concrete blocks mixed by SiO_2 nanoparticles subjected to blast load experimentally and theoretically", *Constr. Build. Mater.*, **174**, 633-644.

Arani, A.J. and Kolahchi, R. (2016), "Buckling analysis of embedded concrete columns armed with carbon nanotubes", *Comput. Concrete*, **17**(5), 567-578.

Asemi, K., Salami, S.J., Salehi, M. and Sadighi, M. (2014), "Dynamic and static analysis of FGM skew plates with 3D elasticity based graded finite element modelling", *Lat. Am. J. Sol. Struct.*, **11**, 504-533.

Attia, A., Bousahla, A.A., Tounsi, A., Mahmoud, S.R. and Alwabli, A.S. (2018), "A refined four variable plate theory for thermoelastic analysis of FGM plates resting on variable elastic foundations", *Struct. Eng. Mech.*, **65**(4), 453-464.

Baferani, A.H., Saidi, A.R. and Jomehzadeh, E. (2012), "Exact analytical solution for free vibration of functionally graded thin annular sector plates resting on elastic foundation", *J. Vibr. Contr.*, **18**(2), 246-267.

Belabed, Z., Bousahla, A.A., Houari, M.S.A., Tounsi, A. and Mahmoud, S.R. (2018), "A new 3-unknown hyperbolic shear deformation theory for vibration of functionally graded sandwich plate", *Earthq. Struct.*, **14**(2), 103-115.

Beldjelili, Y., Tounsi, A. and Mahmoud, S.R. (2016), "Hygro-thermo-mechanical bending of S-FGM plates resting on variable elastic foundations using a four-variable trigonometric plate theory", *Smart Struct. Syst.*, **18**(4), 755-786.

Bellifa, H., Benrahou, K.H., Bousahla, A.A., Tounsi, A. and Mahmoud, S.R. (2017), "A nonlocal zeroth-order shear deformation theory for nonlinear postbuckling of nanobeams", *Struct. Eng. Mech.*, **62**(6), 695-702.

Bellifa, H., Benrahou, K.H., Hadji, L., Houari, M.S.A. and Tounsi, A. (2016), "Bending and free vibration analysis of functionally graded plates using a simple shear deformation theory and the concept the neutral surface position", *J. Braz. Soc. Mech. Sci. Eng.*, **38**(1), 265-275.

Benchohra, M., Driz, H., Bakora, A., Tounsi, A., Bedia, E.A.A. and Mahmoud, S.R. (2018), "A new quasi-3D sinusoidal shear deformation theory for functionally graded plates", *Struct. Eng. Mech.*, **65**(1), 19-31.

Bouderba, B., Houari, M.S.A., Tounsi, A. and Mahmoud, S.R. (2016), "Thermal stability of functionally graded sandwich plates using a simple shear deformation theory", *Struct. Eng. Mech.*, **58**(3), 397-422.

Bouhadra, A., Tounsi, A., Bousahla, A.A., Benyoucef, S. and Mahmoud, S.R. (2018), "Improved HSDT accounting for effect of thickness stretching in advanced composite plates", *Struct. Eng. Mech.*, **66**(1), 61-73.

Bouiadjra, R.B., Mahmoudi, A., Benyoucef, S., Tounsi, A. and Bernard, F. (2018), "Analytical investigation of bending response of FGM plate using a new quasi 3D shear deformation theory: Effect of the micromechanical models", *Struct. Eng. Mech.*, **66**(3), 317-328.

Bousahla, A.A., Benyoucef, S., Tounsi, A. and Mahmoud, S.R. (2016), "On thermal stability of plates with functionally graded coefficient of thermal expansion", *Struct. Eng. Mech.*, **60**(2), 313-335.

Chikh, A., Tounsi, A., Hebali, H. and Mahmoud, S.R. (2017), "Thermal buckling analysis of cross-ply laminated plates using a simplified HSDT", *Smart Struct. Syst.*, **19**(3), 289-297.

Cook, R.D., Malkus, D.S., Plesha, M.E. and Witt, R.J. (2009), *Concepts and Applications of Finite Element Analysis*, John Wiley & Sons, Singapore.

El-Haina, F., Bakora, A., Bousahla, A.A., Tounsi, A. and Mahmoud, S.R. (2017), "A simple analytical approach for thermal buckling of thick functionally graded sandwich plates", *Struct. Eng. Mech.*, **63**(5), 585-595.

Fourn, H., Atmane, H.A., Bourada, M., Bousahla, A.A., Tounsi, A. and Mahmoud, S.R. (2018), "A novel four variable refined plate theory for wave propagation in functionally graded material plates", *Steel Compos. Struct.*, **27**(1), 109-122.

Ghannadpour S.A.M., Ovesy, H.R. and Nassirnia, M. (2012b), "An investigation on buckling behaviour of functionally graded plates using finite strip method", *Appl. Mech. Mater.*, **152**, 1470-1476.

Ghannadpour, S.A.M. and Alinia, M.M. (2006), "Large deflection behavior of functionally graded plates under pressure loads", *Compos. Struct.*, **75**(1-4), 67-71.

Ghannadpour, S.A.M., Ovesy, H.R. and Nassirnia, M. (2012), "Buckling analysis of functionally graded plates under thermal loadings using the finite strip method", *Comput. Struct.*, **108**, 93-99.

Ghannadpour, S.A.M., Ovesy, H.R. and Nassirnia, M. (2012a), "Buckling analysis of functionally graded plates under thermal loadings using the finite strip method", *Comput. Struct.*, **108**, 93-99.

Ghannadpour, S.A.M. and Kiani, P. (2018), "Nonlinear spectral collocation analysis of imperfect functionally graded plates under end-shortening", *Struct. Eng. Mech.*, **66**(5), 557-568.

Gibson, L.J., Ashby, M.F., Karam, G.N., Wegst, U. and Shercliff, H.R. (1995), "Mechanical properties of natural materials. II". *Microstruct. Mech. Efficienc.*, *Proceedings of the Royal Society A*, **450**, 141-162.

Haddadpour, H., Mahmoudkhani, S. and Navazi, H.M. (2007), "Free vibration analysis of functionally graded cylindrical shells including thermal effects", *Thin-Wall. Struct.*, **45**, 591-599.

Hajmohammad, M.H., Farrokhian, A. and Kolahchi, R. (2018), "Smart control and vibration of viscoelastic actuator-multiphase nanocomposite conical shells-sensor considering hygrothermal load based on layerwise theory", *Aerosp. Sci. Technol.*, **78**, 260-270.

Hajmohammad, M.H., Maleki, M. and Kolahchi, R. (2018), "Seismic response of underwater concrete pipes conveying fluid covered with nano-fiber reinforced polymer layer", *Soil Dyn. Earthq. Eng.*, **110**, 18-27.

Hajmohammad, M.H., Azizkhani, M.B. and Kolahchi, R. (2018), "Multiphase nanocomposite viscoelastic laminated conical shells subjected to magneto-hygrothermal loads: Dynamic buckling analysis", *Int. J. Mech. Sci.*, **137**, 205-213.

Huang, X.L. and Shen, H.S. (2004), "Nonlinear vibration and dynamic response of functionally graded plates in thermal environments", *Int. J. Sol. Struct.*, **41**, 2403-2427.

Kar, V.R. and Panda, S.K. (2015), "Free vibration responses of temperature dependent functionally graded doubly curved panels under thermal environment", *Lat. Am. J. Sol. Struct.*, **12**(11), 2006-2024.

Karami, B., Janghorban, M. and Tounsi, A. (2018), "Nonlocal strain gradient 3D elasticity theory for anisotropic spherical nanoparticles", *Steel Compos. Struct.*, **27**(2), 201-216.

Karami, B., Janghorban, M. and Tounsi, A. (2018), "Variational approach for wave dispersion in anisotropic doubly-curved nanoshells based on a new nonlocal strain gradient higher order shell theory", *Thin-Wall. Struct.*, **129**, 251-264.

Karami, B., Janghorban, M., Shahsavari, D. and Tounsi, A. (2018), "A size-dependent quasi-3D model for wave dispersion analysis of FG nanoplates", *Steel Compos. Struct.*, **28**(1), 99-110.

Kiani, Y., Dimitri, R. and Tornabene, F. (2018), "Free vibration of FG-CNT reinforced composite skew cylindrical shells using Chebyshev-Ritz formulation", *Compos. Part B Eng.*, **147**, 169-177.

Koizumi, M. (1993), "The concept of FGM, ceramic transactions, functionally gradient materials", **34**, 3-10.

Kolahchi, R. (2017), "A comparative study on the bending, vibration and buckling of viscoelastic sandwich nano-plates based on different nonlocal theories using DC, HDQ and DQ methods", *Aerosp. Sci. Technol.*, **66**, 235-248.

Kolahchi, R. and Bidgoli, A.M. (2016), "Size-dependent sinusoidal beam model for dynamic instability of single-walled carbon nanotubes", *Appl. Math. Mech.*, **37**(2), 265-274.

Kolahchi, R. and Cheraghbak, A. (2017), "Agglomeration effects on the dynamic buckling of viscoelastic microplates reinforced with SWCNTs using Bolotin method", *Nonlin. Dyn.*, **90**(1), 479-492.

Kolahchi, R., Hosseini, H. and Esmailpour, M. (2016), "Differential cubature and quadrature-Bolotin methods for dynamic stability of embedded piezoelectric nanoplates based on visco-nonlocal-piezoelasticity theories", *Compos. Struct.*, **157**, 174-186.

Kolahchi, R., Safari, M. and Esmailpour, M. (2016), "Dynamic stability analysis of temperature-dependent functionally graded CNT-reinforced visco-plates resting on orthotropic elastomeric medium", *Compos. Struct.*, **150**, 255-265.

Kolahchi, R., Zarei, M.S., Hajmohammad, M.H. and Nouri, A. (2017), "Wave propagation of embedded viscoelastic FG-CNT-reinforced sandwich plates integrated with sensor and actuator based on refined zigzag theory", *Int. J. Mech. Sci.*, **13**, 534-545.

Kolahchi, R., Zarei, M.S., Hajmohammad, M.H. and Oskouei, A. N. (2017), "Visco-nonlocal-refined Zigzag theories for dynamic buckling of laminated nanoplates using differential cubature-Bolotin methods", *Thin-Wall. Struct.*, **113**, 162-169.

Mehrparvar, M. and Ghannadpour, S.A.M. (2018), "Plate assembly technique for nonlinear analysis of relatively thick functionally graded plates containing rectangular holes subjected to in-plane compressive load", *Compos. Struct.*

Menasria, A., Bouhadra, A., Tounsi, A., Bousahla, A.A. and Mahmoud, S.R. (2017), "A new and simple HSDT for thermal stability analysis of FG sandwich plates", *Steel Compos. Struct.*, **25**(2), 157-175.

Mokhtar, Y., Heireche, H., Bousahla, A.A., Houari, M.S.A., Tounsi, A. and Mahmoud, S.R. (2018), "A novel shear deformation theory for buckling analysis of single layer graphene sheet based on nonlocal elasticity theory", *Smart Struct. Syst.*, **21**(4), 397-405.

Mouffoki, A., Bedia, E.A., Houari, M.S.A., Tounsi, A. and Mahmoud, S.R. (2017), "Vibration analysis of nonlocal advanced nanobeams in hygro-thermal environment using a new two-unknown trigonometric shear deformation beam theory", *Smart Struct. Syst.*, **20**(3), 369-383.

Ovesy, H.R. and Ghannadpour, S.A.M. (2007), "Large deflection finite strip analysis of functionally graded plates under pressure loads", *Int. J. Struct. Stab. Dyn.*, **7**(2), 193-211.

Ovesy, H.R., Ghannadpour, S.A.M. and Nassirnia, M. (2015), "Post-buckling analysis of rectangular plates comprising functionally graded strips in thermal environments", *Comput. Struct.*, **147**, 209-215.

Patel, B.P., Gupta, S.S., Loknath, M.S. and Kadu, C.P. (2005), "Free vibration analysis of functionally graded elliptical cylindrical shells using higher-order theory", *Compos. Struct.*, **69**, 259-270.

Pathak, P., Zhang, Y.X. and Teng, X. (2016), "Nonlinear finite element analysis of FRP strengthened RC beams with bond-slip effect", *Int. J. Comput. Meth.*, **14**(3), 1750032.

Pradyumna, S. and Bandyopadhyay, J.N. (2008), "Free vibration analysis of functionally graded curved panels using a higher-order finite element formulation", *J. Sound Vibr.*, **318**, 176-192.

Pradyumna, S. and Bandyopadhyay, J.N. (2010), "Free vibration and buckling of functionally graded shell panels in thermal environments", *Int. J. Struct. Stab. Dyn.*, **10**(5), 1031-1053.

Reddy, J.N. and Chin, C.D. (1998), "Thermomechanical analysis of functionally graded cylinders and plates", *J. Therm. Stress.*, **21**, 593-626.

Reddy, J.N. (2004), *Mechanics of Laminated Composite: Plates and Shells-Theory and Analysis*, CRC Press, Boca Raton.

Santos, H., Soares, C.M.M., Soares, C.A.M. and Reddy, J.N. (2009), "A semi-analytical finite element model for the analysis of cylindrical shells made of functionally graded materials", *Compos. Struct.*, **91**, 427-432.

Shen, H.S. (2009), *Functionally Graded Material: Nonlinear Analysis of Plates & Shells*, CRC Press, Boca Raton.

Shen, H.S. and Wang, H. (2014), "Nonlinear vibration of shear deformable FGM cylindrical panels resting on elastic foundations in thermal environments", *Compos.: Part B*, **60**, 167-177.

Sherafat, M.H. and Ovesy, H.R. (2013), "Buckling analysis of functionally graded plates under mechanical loading using higher order functionally graded strip", *Int. J. Struct. Stab. Dyn.*, **13**(6).

Sundararajan, N., Prakash, T. and Ganapathi, M. (2005), "Nonlinear free flexural vibrations of functionally graded rectangular and skew plates under thermal environments", *Fin. Elem. Analy. Des.*, **42**, 152-168.

Taj, G. and Chakrabarti, A. (2013), "Dynamic response of functionally graded skew shell panel", *Lat. Am. J. Sol. Struct.*, **10**, 1243-1266.

Talha, M. and Singh, B.N. (2011), "Large amplitude free flexural vibration analysis of shear deformable FGM plates using nonlinear finite element method", *Fin. Elem. Analy. Des.*, **47**, 394-401.

Uymaz, B. and Aydogdu, M. (2007), "Three-dimensional vibration analysis of functionally graded plates under various boundary conditions", *J. Reinf. Plast. Compos.*, **26**(18), 1847-1863.

Yazid, M., Heireche, H., Tounsi, A., Bousahla, A.A. and Houari, M.S.A. (2018), "A novel nonlocal refined plate theory for stability response of orthotropic single-layer graphene sheet resting on elastic medium", *Smart Struct. Syst.*, **21**(1), 15-25.

Younsi, A., Tounsi, A., Zaoui, F.Z., Bousahla, A.A. and Mahmoud, S.R. (2018), "Novel quasi-3D and 2D shear deformation theories for bending and free vibration analysis of FGM plates", *Geomech. Eng.*, **14**(6), 519-532.

Yousfi, M., Atmane, H.A., Meradjah, M., Tounsi, A. and Bennai, R. (2018), "Free vibration of FGM plates with porosity by a shear deformation theory with four variables", *Struct. Eng. Mech.*, **66**(3), 353-368.

Zarei, M.S., Kolahchi, R., Hajmohammad, M.H. and Maleki, M. (2017), "Seismic response of underwater fluid-conveying concrete pipes reinforced with SiO_2 nanoparticles and fiber reinforced polymer (FRP) layer", *Soil Dyn. Earthq. Eng.*, **103**, 76-85.

Zhao, X., Lee, Y.Y. and Liew, K.M. (2009), "Free vibration analysis of functionally graded plates using the element-free kp-Ritz method", *J. Sound Vibr.*, **319**, 918-939.

Zhu, P., Zhang, L.W. and Liew, K.M. (2014), "Geometrically nonlinear thermomechanical analysis of moderately thick functionally graded plates using a local Petrov-Galerkin approach with moving Kriging interpolation", *Compos. Struct.*, **107**, 298-314.

Zine, A., Tounsi, A., Draiche, K., Sekkal, M. and Mahmoud, S.R. (2018), "A novel higher-order shear deformation theory for bending and free vibration analysis of isotropic and multilayered plates and shells", *Steel Compos. Struct.*, **26**(2), 125-137.

CC